Carbon Nanotube Electronics and Optoelectronics

Ph. Avouris*, A. Afzali, J. Appenzeller, J. Chen, M. Freitag, C. Klinke, Y.-M. Lin, J.C. Tsang
IBM T. J. Watson Research Center, Yorktown Heights, NY 10598
Tel: (914) 945-2722, Fax: (914) 945-4531, e-mail: avouris@us.ibm.com

Abstract

We discuss recent developments in our research on single carbon nanotube field-effect transistors and light emitting and detecting devices. Specifically, we show that by using either double gate devices, or selective charge-transfer doping, we can convert Schottky barrier CNTFETs into bulk-switched devices, ambipolar CNTFETs into unipolar devices, while at the same time enhance both the ON and OFF state device characteristics. Under ambipolar conditions CNTFETs can be used as light emitters via e-h recombination, while light irradiation of CNTFETs leads to photoconductivity. Thus, the CNTFET can be used as a high performance switch, a light source and a light detector.

Introduction

We have been working to understand the switching mechanism, and scaling behavior and to enhance the performance of carbon nanotube field-effect transistors. (CNTFETs). [1,2] In earlier work we determined that, in general, Schottky barriers (SB) develop at the metal source (drain)/nanotube junctions and that the anomalous sub-threshold characteristics of the transistor (large sub-threshold slope, *S*) and certain aspects of the influence of the ambient on the transistor, such as the sensitivity to oxygen, can be understood in terms of the SB model [1,2]. Recently, we showed [3] that vertical scaling, i.e., thinning of the gate oxide, of unipolar CNTFETs converts them to ambipolar devices.

Field-effect transistors

The transfer characteristics of an ambipolar device are shown in Fig. 1. It is seen that as the drain bias is increased the leakage current also increases and the ON/OFF current ratio decreases. [3] Such behavior is undesirable in logic applications and must be avoided. However, we found that the ambipolar character of CNTFETs can be particularly valuable in optoelectronic applications.

One way to eliminate the ambipolar behavior of CNTFETs is by gate engineering. [4 Heinze APL] We have demonstrated this approach by fabricating a trench near the drain of CNTFETs thus producing a unipolar device due to the weaker gating near the drain. [5 Lin]. However, the sub-threshold swing of the device remained high.

Here we report on strategies that allow the conversion of a SB-CNTFET into a bulk-switched FET, eliminating the ambipolar character, while simultaneously improving both the ON and OFF state characteristics of the FET. We used two different approaches to achieve these goals: (a) one involves the electrostatic doping of the metal/nanotube contacts using double gate device structure [6], (b) while the other employs charge-transfer doping of the contacts by adsorbed molecular species. [7] In both cases the goal is to suppress ambipolar behavior and produce a bulk-switched device. Fig. 2 shows the structure of a double gate CNTFET. [6] Adjacent to the source and drain electrodes are two regions labeled A that can be back-gated through the Si wafer. A second gate made of aluminum is fabricated at the center of the device and is partially oxidized to give a 10 nm Al_2O_3 gate insulator. The CNT is placed on top of this structure. Subsequently, an HSQ resist layer on top of the structure is used to pattern the underlying Al gate (region B) and obtain self-alignment with respect to region A. When the silicon

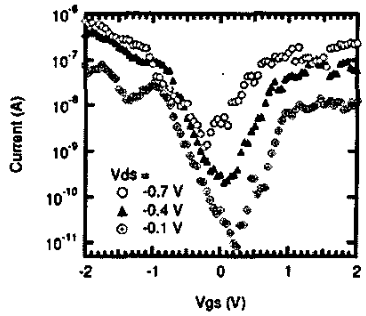

Fig. 1. Transfer characteristics of an ambipolar CNTFET. The CNT has a diameter of ~1.4 nm, and the gate oxide (SiO_2) is 10nm thick. Note the deteriorating characteristics with increasing Vds.

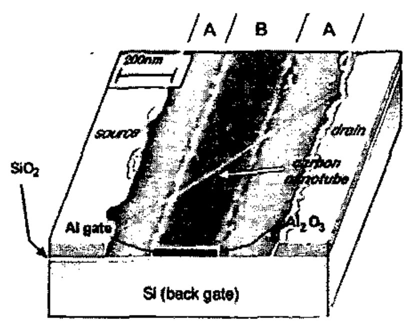

Fig. 2. An SEM image of a double-gate CNTFET. The CNT diameter is ~ 1.4 nm and the thickness of SiO_2 is 10 nm. An Al metal film (20-nm thick) is placed underneath the nanotube to act as a second gate, with a layer of 4-nm-thick Al_2O_3 as the gate oxide. The areas between the Al gate and the source/drain that are gated by the Si wafer are denoted as regions A, and the Al gate is denoted as region B.

0-7803-8684-1/04/$20.00 ©2004 IEEE

back-gate bias $V_{g\text{-}Si}$ is set equal to the Al gate $V_{g\text{-}Al}$ bias, the expected ambipolar behavior is observed. When $V_{g\text{-}Al}$=0, the current of the device is not affected indicating that this gate does not influence the contacts. By applying a $V_{g\text{-}Si}<0$ a p-i-p structure is formed (Fig. 3), while for $V_{g\text{-}Si}>0$ (not shown) an n-i-n structure is formed. In this arrangement, regions A act simply as extensions of the source and drain, they suppress the SBs and produce a bulk-switched device (Fig. 3).

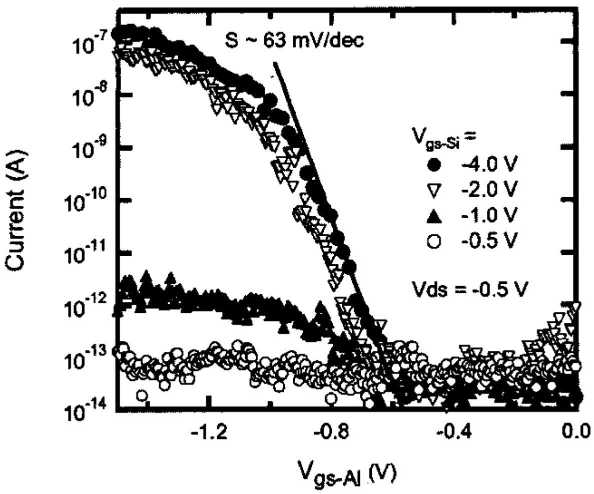

Fig. 3 Drain current vs. Al gate voltage of a double gate CNTFET for different voltages of the Si back-gate. Vds was kept at –0.5V.

The qualitative band diagram in Fig. 4 illustrates the operation of the p-i-p and n-i-n double gate devices. The p-type double gate device has a drastically improved sub-threshold swing S~65 mV/decade, close to the theoretical limit of ~ 60 mV/dec at room temperature. For comparison, the same device exhibits S ~ 100 mV/dec when operated as a SB-CNFET. Finally, Fig. 5 shows the measured I_d vs. $V_{g\text{-}Al}$ curves for different drain voltages at $V_{g\text{-}Si}$ = -4 V. Unlike the ambipolar device in Fig. 1, there is no impact of V_{ds} on I_d leading to excellent DIBL device performance. [6]

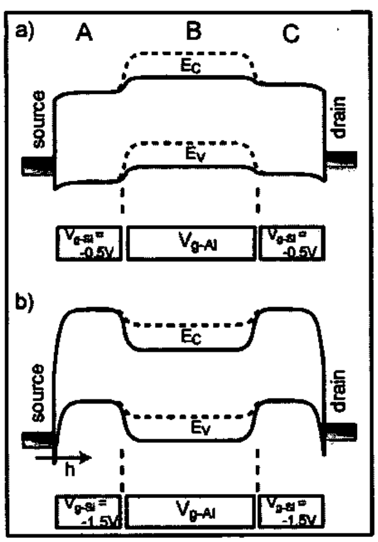

Fig. 4 Qualitative band diagram of the double gate CNTFET shown in Fig. 2. (a) For Vg-Si= -0.5V and (b) for Vg-Si= -1.5V. Solid and dashed lines represent the band-bending in region B for two different values of Vg-Al.

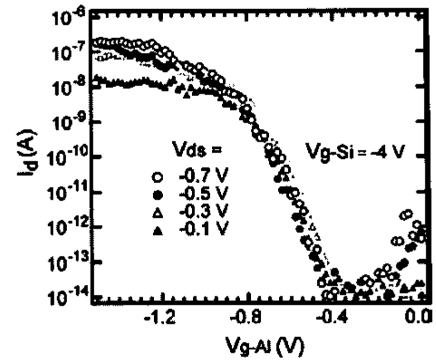

Fig. 5. Drain current of the double gate CNTFET vs. Al-gate bias for several values of the drain bias. The Si back-gate bias was fixed at –4V.

An alternate solution of the above problems involves chemical doping. [7] Since substitutional doping has not been demonstrated in CNTs and ion implantation is not useful since it destroys the nanotube lattice, we have utilized the charge-transfer process from adsorbed molecules. The doping itself may involve the entire device, i.e. both channel and contacts, or certain areas of the device can be selected for doping using masking techniques. As a stable p-dopant we use triethyloxonium-hexachloro-antimonate ($(C_2H_5)_3O^+SbCl_6^-$), which will be referred to as **OA**. Each **OA** molecule can remove one electron from the nanotube. Left behind are $SbCl_6^-$ counter ions, while the remaining species of the reaction are volatile products. The doping is performed by simply immersing the CNT in a solution of **OA** in dichlorobenzene. Selective doping is achieved by protecting the parts of the device not to be doped using a film of HSQ resist. Figure 6 shows the transfer characteristics at V_{ds}=-0.5V of a CNTFET with a gate oxide thickness of t_{ox}=10nm. Initially the transistor was ambipolar, but after doping with **OA** it shows strong p-character. The threshold voltage, V_{th}, for hole conduction increased from –1.55V to –0.85V, and the ON state current, I_{on}, at constant overdrive, increased by about two orders of magnitude. [7] The sub-threshold characteristics also improved, with the sub-threshold swing S decreasing from 120mV/dec to 85mV/dec upon **OA** doping. We believe that the above findings can be explained in terms of (a) p-doping of the CNT and (b) the modification of the work-function (Φ) of the source and drain electrodes and, therefore, of the corresponding Schottky barriers. The modification of Φ involves the adsorption of the $SbCl_6^-$ ions, which, with the induced image charge in the metal, produce an outward directed dipole that increases Φ. This increase favors hole injection at one electrode, while suppressing electron injection at the other. The important role of the SBs can be seen in Fig. 7 which shows the improvement of the ON and OFF state characteristics of a CNTFET after doping only the contact region with **OA**. At sufficiently high doses of **OA** the CNT can become degenerate with little effect of the gate on its conductance. [7]

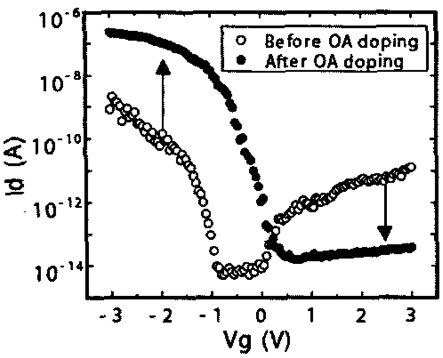

Fig. 6. Transfer characteristics of a CNFET with Pd electrodes and tox= 10 nm before and after doping with **OA**. Vds= -0.5V.

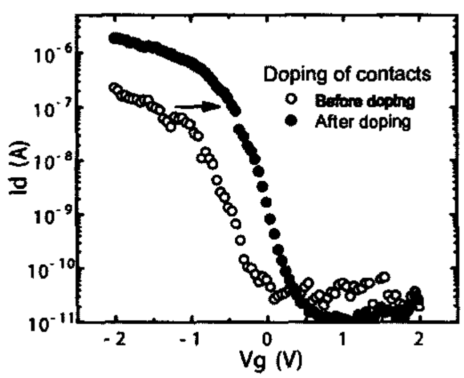

Fig 7. The effects of selective p-doping with **OA** of the region of the source/drain-CNT contacts of a CNTFET.

One particularly interesting interaction that leads to p-doping involves the protonation of CNTs by solid state organic, or inorganic acids. In figure 8 we show the transfer characteristics of a CNTFET before and after a film of perfluorododecanoic acid has been deposited on it (Fig. 8). Both a threshold shift and current increase are observed. It is not clear how the proton transfer from the acid to the CNT proceeds, i.e., if a sigma-type (phenonium-like), or a pi-type structure is formed. The estimated hole-doping in Fig. 7 is about 0.1 h/nm corresponding to ~10^{19} h/cm^3. N-type charge transfer doping is also possible. Amines possessing the lone pair of electrons on the nitrogen atom are particularly efficient electron donors. Using hydrazine (N_2H_4) n-doping densities as high as 0.5e/nm (~ 10^{20} e/cm^3 in 3D) were thus achieved [8].

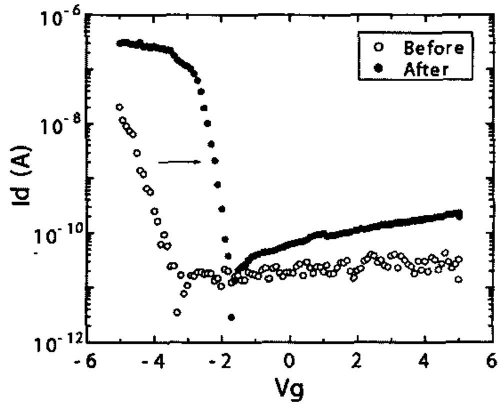

Fig. 8. The effect of p-doping of a CNTFET with pefluorododecanoic acid ($CF_3(CF_2)_{10}CO_2H$) upon its transfer characteristics. Source and drain made of Pd, gate oxide 20 nm, Vds= -0.5V.

Charge-transfer doping can also be used to achieve the same results as the double gate device described above. For this purpose a top-gated CNTFET is fabricated on a thickly oxidized Si wafer. The metal gate is designed so as not to cover the nanotube near the source and drain electrodes leaving gaps of the order of 30-50nm. Under these conditions the gate cannot turn-on the CNTFET. However, after the exposed length of the CNT as well as the CNT-source/drain interfaces are chemically doped with OA, a unipolar FET with good ON and OFF state characteristics is formed [7].

Optoelectronics

Unlike silicon, semiconductor nanotubes are direct gap 1D semiconductors, readily absorb and emit light and, therefore, have the potential for applications in optoelectronics. [1] In particular, using ambipolar CNTFETs with appropriate biasing we can inject simultaneously electrons and holes from the source and drain of the nanotube. The confined electrons and holes will recombine and one of the possible recombination channels is radiative recombination. We have tested this possibility using a liquid nitrogen cooled HgCdTe IR camera. Indeed we observed IR radiation originating from the CNT channel of an ambipolar CNTFET. [9] The radiation was polarized along the CNT axis, and for a given V_{ds} it was maximized when $V_{gs}=V_{ds}/2$. This observation is in agreement with the expectation that, for a symmetric device structure, the electron and hole currents will be equal maximizing the light intensity. [3] Using a filter array we were able to record the electroluminescence spectra from individual CNTs, and

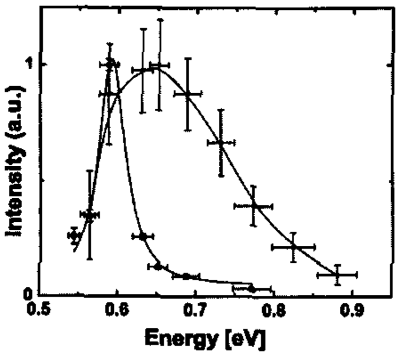

Fig. 9. Electroluminescence spectra from two single-nanotube CNTFETs. The narrow width spectrum arises from a long nanotube (>5μm), while the broad emission is obtained with a short (~300nm) nanotube.

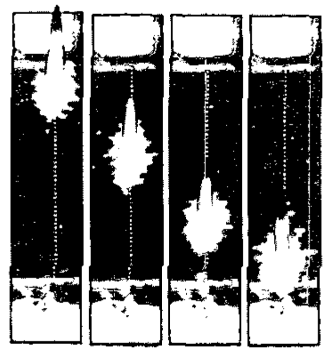

Fig. 10. Controlling the position of the emission spot along the channel of a long (50μm) CNTFET by varying the gate voltage under constant drain current conditions.

found them to be in agreement with photoluminescence spectra. However, the lineshape of the peaks in the electroluminescence spectra show dependence on the length of the CNT and the value of the current. Fig. 9 shows electroluminescence spectra from two individual CNTFETs with widely different channel lengths, but similar currents [3]. The long channel device (L≥5μm) gives narrow, rather symmetric peaks, while the short channel (~300nm) device gives broad, asymmetric spectra. [10] We have shown that the emission lineshapes reflect the energy distribution of the carriers in the channel of the CNTFET. For the short CNTs we extracted a broad distribution with a cut off at ~180meV. The distribution is determined by the residence time of the carriers in the CNT and the phonon scattering rates, which are dominated by fast relaxation via the optical phonon at ~180meV. [11,12]

We see that the CNTFETs provides a novel form of molecular light source. Unlike LEDs, which involve chemical doping and a well defined space charge region, CNTFETs do not require doping. Most importantly, we find that the gate of the CNTFET allows the tuning of not only the intensity of the emission, but also its position along the length of the CNT from which the emission originates. [13] Fig. 10 shows an IR image of a set of source and drain electrodes bridged by a long CNT (not visible). The Si wafer acts as the back-gate. Superimposed on this image we show the movement of the emission spot from e-h recombination as the gate voltage is scanned while maintaining a constant current. By varying V_{gs} the recombination region can be translated over large distances (tens of microns) in long CNTs. [13] Such spatially-resolved measurements can provide new insights into the transport processes in CNTs. They allow us to follow the fronts of the electron and hole currents under varying bias conditions, *determine the recombination lengths and recombination* times and other transport properties. Another interesting observation involves the appearance of stationary emission spots in parts of the CNT where transport is unipolar. [13] This implies that the particular spots are sources of both carriers. The intensity of stationary light spots increases when the traveling spot is near them, i.e., when the local electric field is high. Fig. 11 shows the spatial location of the light spot as Vds is scanned from -40V to 0V and back to -15V. (This particular device shows strong asymmetry, hysteresis, due to charge trapping during the scan.) A number of static emission spots appear as parallel lines. [13] The strong dependence on the E-field suggests local Zener tunneling and/or avalanching processes. The emission near the electrodes where high fields are present also shows an enhancement.

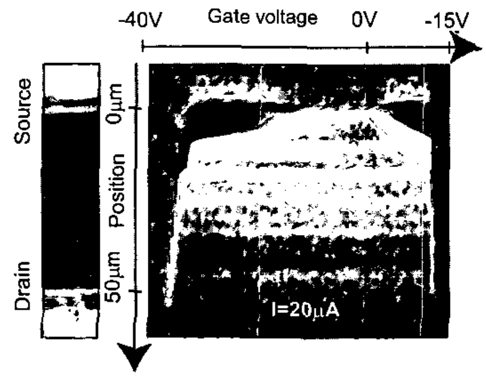

Fig. 11. The position of the light emission spot as a function of the gate voltage. (Id=20μA). Emissions from several static points is observed that appear as lines parallel to the voltage axis

In addition to electrically excited light emission from individual nanotubes, we have demonstrated the reverse process, i.e., photocurrent generation in single nanotubes. [14] The confinement of the electron and hole in CNTs leads to strong e-h coupling and the formation of excitons which dominate the absorption spectra of nanotubes. [15,16] We use a Ti Sapphire laser to excite the second excited state of nanotubes (usually designated as the E_{22} state) whose dissociation in the applied E-field produces the photocurrent. [15] Fig. 12 shows a photocurrent excitation spectrum of a CNT. The main peak at 1.35eV corresponds to the energy of the second exciton state, while the sideband at ~180meV higher energy could arise from the excitation of an optical phonon mode of the CNT [17], or be the second inter-band transition (E_{22}). From the technological point of view the quantum efficiency, ϕ, of the CNTs as a photon detector is very important. Expressed as e-h pairs per absorbed photon we estimate ϕ to be quite high ~10%. [14] Photo-voltage from single CNTs can also be detected and Figure 13 shows an example.

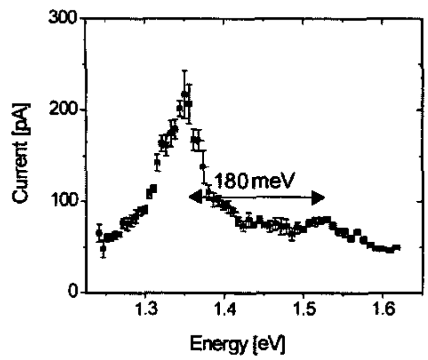

Fig. 12. Photoconductivity spectrum of a single CNTFET. The main peak at ~1.35eV corresponds to the second exciton peak of the CNT, while the side band at about 180meV higher energy which correlates with the excitation of one quantum of an optical phonon mode, or the 2nd interband transition .

In conclusion, we find that CNTFETs are particularly promising not only as high performance transistors, but also hold promise for optoelectronic applications as IR light emitters and detectors. Of course, many critical problems must be solved before we can determine if a CNT-based nanotechnology can be developed.

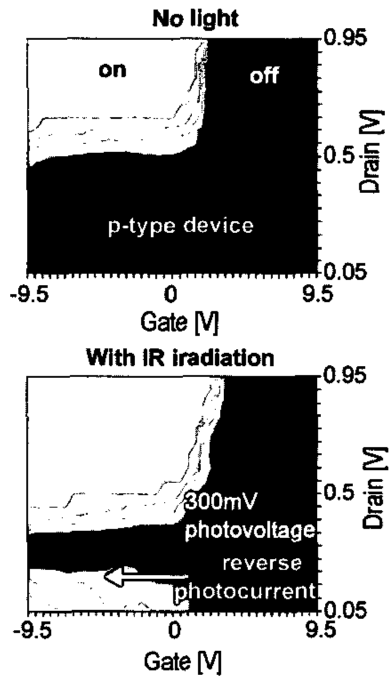

Fig. 13. Photovoltage generation in single CNTFETs. Top: Transfer characteristics of a p-type CNTFET in the dark. Bottom: transfer characteristics of the same CNTFET upon IR irradiation.

References

[1] Ph. Avouris, MRS Bulletin **29**, 403 (2004).

[2] Ph. Avouris, J. Appenzeller, R. Martel, and S. Wind, Proc. IEEE **91**, 1772 (2003).

[3] M. Radosavljevic, S. Heinze, J. Tersoff, and Ph. Avouris, Appl. Phys. Lett. **83**, 2435 (2003).

[4] S. Heinze, J. Tersoff and Ph. Avouris, Appl. Phys. Lett. **83**, 5038 (2003).

[5] Y.-M. Lin, J. Appenzeller, and Ph. Avouris, Nano Letters **4**, 947 (2004).

[6] Y.-M. Lin, J. Appenzeller, J. Knoch and Ph. Avouris, IEEE Trans. Nanotech., submitted.

[7] J. Chen, C. Klinke, A. Afzali, and Ph. Avouris, Appl. Phys. Lett., submitted.

[8] J. Chen, C. Klinke, A. Afzali, and Ph. Avouris, Nano Letters, submitted.

[9] J.A. Misewich, R. Martel, Ph. Avouris, J.C. Tsang, S. Heinze and J. Tersoff, Science **300**, 783 (2003).

[10] M. Freitag, V. Perebeinos, J. Chen, A. Stein, J. Misewitch, R. Martel, and Ph. Avouris, Nano Letters **4**, 1063 (2004).

[11] A. Javey, J. Guo, Q. Wang, M. Landstrom, and H. Dai, Nature **424**, 654 (2003).

[12] V. Perebeinos, J. Tersoff and Ph. Avouris, unpublished.

[13] M. Freitag, J. Chen, J. Tersoff, J. Tsang, Q. Fu, J. Liu, Ph. Avouris, Phys. Rev. Lett. 93, 076803 (2004).

[14] M. Freitag, Y. Martin, J.A. Misewich, R. Martel, and Ph. Avouris. **3**, 1067 (2003).

[15] C. D. Spataru, S. Ismail-Beigi, L.X. Benedict, and S. G. Louie, Phys. Rev. Lett. **92**, 077402 (2004).

[16] V. Perebeinos, J. Tersoff and Ph. Avouris, Phys. Rev. Lett. **92**, 257402 (2004).

[17] V. Perebeinos, J. Tersoff, and Ph. Avouris, submitted for publication.